中正嶺學報 第三十六卷 第一期 民國 96.11.
JOURNAL OF C.C.I.T., VOL. 36, NO. 1, Nov, 2007

Numerical Studies on Crack Dilatancy of Concrete I: Model Establishment and Verification

Tsai-Fu Chuang

Department of Landscape Architecture, MingDao University

ABSTRACT

In this paper, a simple smeared crack dilatancy model is proposed. This model assumed that by increasing the shear slip, a certain amount of volumetric increase would be caused. This leads to either free expansion or an increase in the compressive stress if confined. In such a way, the dilatancy effect could be simulated by considering the amount of volumetric change or the change in compressive stress in confined conditions. Three crack dilatancy diagrams have been used to estimate the values of dilatancy parameters. The above dilatancy parameters were then selected and implemented into the open crack state. A single element test is designed to evaluate the performance of the simple dilatancy model. In this test, two state displacement controls were adopted to investigate the characteristics of the simple dilatancy model. The numerical test provided a logical result and this indicates that the simple dilatancy model is able to properly estimate the influence of the dilatancy effect and can be employed in a more complex structure.

Keywords: Dilatancy, Smeared crack model, Finite element method

混凝土裂縫膨脹性的數值模擬分析 Ⅰ:模式建立與驗證

莊財福

明道大學造園景觀系助理教授

摘要

在這篇文章裡，提出一個簡單的混凝土均散裂縫膨脹模式（smeared crack dilatancy model）。本模型假設在增加剪力滑移（shear slip）的條件下，將產生一定大小的體積增量，且將導致混凝土自由膨脹。但如果在邊界被限制的狀況之下，則將引起一定量的體積增量。如此一來，則混凝土膨脹性（dilatancy）的效用可透過考量體積的變化量或壓力的改變量（在限制的邊界條件裡）被間接考量。本研究並採用三組裂縫膨脹曲線去估算混凝土膨脹參數的值。上述參數並接著被考慮於完全開縫狀態（open crack stagte）。本研究並設計一組單一元素測試（Single element test）以評估本模型的各項性能。測試結果顯示本模式對於估計混凝土膨脹性的效用具有相當的合理性。

關鍵詞：膨脹，塗抹裂縫模式，有限元素法

文稿收件日期 95.12.04；文稿修正後接受日期 96. 8.10
Manuscript received December 04, 2006; revised August 10, 2007

I. INTRODUCTION

A very early finite element codes to model the crack behaviour of concrete was that proposed by Bazant and Cedolin [1]. They also proposed a fracture energy criterion to analyse a rectangular reinforced concrete panel for crack propagation. Furthermore, they also explained the reason for the "mesh dependence". The explanation given for this spurious mesh sensitivity, or inobjectivity, was that the value of the stress in an element ahead of a crack front depends on the width of the crack band. Also, the width depends on the element size because the crack width is the effective width of the area or volume associated with a particular element sampling point. Thus, the smaller the elements, the sharper the cracks and the higher the stress in the element ahead of the crack tip.

The methods proposed by Bazant and Cedolin [1] drew attention to the fracture energy and suggested that the answer to the spurious mesh sensitivity was to apply fracture mechanics.

Doubtless, these were problems that could be overcome, and, a fracture energy dependent softening model was then proposed by Bazant and Oh [2] for application to the smeared crack model. They suggested that cracks occurred in a band or zone rather than a line, and also, that over the zone, a fracture strain could be defined which was equal to the sum of the openings of the individual micro-cracks divided by the width of the fracture process zone. Thus, their crack criterion for governing the crack initiation was again assumed to be the tensile strength and once a crack had started, the stress was then followed by a decreasing linear function of the increasing fracture strain. The fracture energy, per unit area of crack, could then be equated to the area under the stress/fracture strain curve multiplied by the width of the fracture process zone. In the smeared crack approach, a crack is assumed to be spread over the width associated with a sampling position and thus the 'numerical' crack process zone was assumed to depend upon the size of the element. Bazant and Oh [2] simply equated the 'characteristic length' of an element with the width of the crack process zone.

This model was rapidly adopted by other investigators [3-5] and become a well-established way of modelling concrete fracture and this approach is also adopted in this paper.

In reinforced concrete, it is well known that shear forces in cracks are transferred by a combination of dowel action and aggregate interlock. The last phenomenon, in particular, is often assumed to contribute significantly to the shear forces [6].

Qualitatively, it is understood that, during shear motion of a crack, opening of the crack (dilatancy) due to the uneveness of the crack surfaces will also occur and if the opening is restrained then a compressive stress is introduced on the crack surface. Indeed, a good deal of research has been conducted in the past two decades to collect more experimental data on the topic [7,8]. Also, many formulas have been proposed to capture this phenomenon analytically, e.g., Gambarova and Karakoc [9], and Walraven and Reinhardt [8].

Feenstra et al. [6] implemented these crack dilatancy formulas into the finite element code in their discrete crack model. Because of lack of experimental data, they ignored the effect of shear normal coupling (crack dilatancy) in the crack development state and assumed that this effect was only of importance in the open crack state.

Chan et al. [10] carried out a preliminary numerical study on smeared dilatancy model. Because of lack of experimental data, they assumed a theoretical criterion to calculate the effect of shear normal coupling in the crack development state. In this study, the opening of the crack (dilatancy) due to the uneveness of the crack surfaces has been considered.

In this paper, the author developed a simple smeared crack model that takes into account of the crack dilatancy in order to investigate the influence of dilatancy effect in an entire structure. In addition, various dilatancy experimental data [8,9,11] are collected from the literature in order to calibrate the dilatancy model.

II. METHOD OF ANALYSIS

The basic fracture model used is the "smeared fixed crack model" which has a maximum tensile stress criterion for initial crack formation and subsequently the concrete is treated as orthotropic with the material strain softening in the direction normal to the crack. In this study, a flat stepped softening curve was proposed based on that suggested by Nilsson and Oldenburg [12]

(Fig. 1).

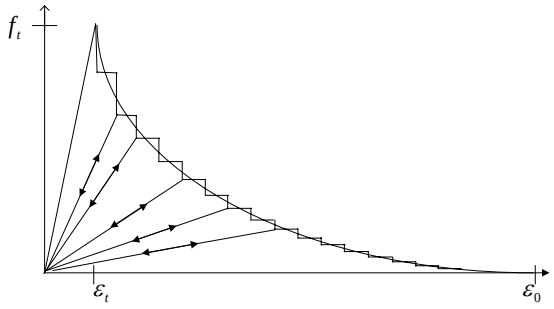

Fig. 1. Flat stepped softening curve for tension

The shear modulus G, in the cracked D-matrix, is multiplied by a shear retention factor β (Fig. 2).

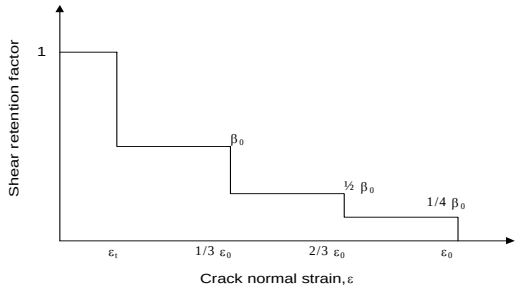

Fig. 2. shear retention factor

The cracked compliance matrix for a single crack is

$$\begin{bmatrix} \Delta\varepsilon_{11} \\ \Delta\varepsilon_{22} \\ \Delta\gamma_{12} \end{bmatrix} = \begin{bmatrix} 1/D_1 & 0 & 0 \\ 0 & 1/D_2 & 0 \\ 0 & 0 & 1/\beta G \end{bmatrix} \begin{bmatrix} \Delta\sigma_{11} \\ \Delta\sigma_{22} \\ \Delta\tau_{12} \end{bmatrix} \quad (1)$$

Hence the D matrix can be represented as

$$\mathrm{D_{cr}} = \begin{bmatrix} D_1(\varepsilon_{11}) & 0 & 0 \\ 0 & D_2(\varepsilon_{22}) & 0 \\ 0 & 0 & \beta G \end{bmatrix} \quad (2)$$

where $D_1(\varepsilon_{11})$ and $D_2(\varepsilon_{22})$ are derived from the slope of the softening curve.

$D_1(\varepsilon_{11})$ = Tangential stiffness modulus in 1 direction i.e. normal to the crack plane.

$D_2(\varepsilon_{22})$ = Tangential stiffness modulus in 2 direction i.e. perpendicular to 1 direction.

β = Shear retention factor which is a function of the normal crack strain (ε_1 or ε_2).

G = Elastic shear modulus.

ε_{11} = Total fracture strain in 1 direction i.e. normal to the crack plane.

ε_{22} = Total fracture strain in 2 direction i.e. perpendicular to 1 direction.

$\Delta\varepsilon_{11}$ = Concrete strain increment in 1 direction i.e. normal to the crack plane.

$\Delta\varepsilon_{22}$ = Concrete strain increment in 2 direction i.e. perpendicular to 1 direction.

$\Delta\gamma_{12}$ = Shear strain increment.

$\Delta\sigma_{11}, \Delta\sigma_{22}$ = Principal stress increments.

$\Delta\tau_{12}$ = Shear stress increment.

The mode I fracture energy can be derived by multiplying the area under the σ-ε curve with the characteristic length l_e. Therefore, the mode I fracture energy G_f can be represented as follows:

$$\mathrm{G_F} = l_e \int_0^{\varepsilon_0} \sigma d\varepsilon = l_e \times \text{area under the curve} \quad (3)$$

where l_e = characteristic length and is taken as the cubic root of the volume associated with an element sampling point. G_F = Fracture energy per unit area; ε_0 = ultimate fracture strain; ε_t = elastic ultimate strain.

In the current study, the equations of the softening curve (Fig. 1) suggested by Nilsson and Oldenburg [12] is shown as bellows:

$$\sigma = \mathrm{f_t} \times \exp\left(\frac{\varepsilon_t - \varepsilon}{\alpha}\right) \quad (4)$$

$$\alpha = (\mathrm{G_F} - 0.5 \times \mathrm{f_t} \times \varepsilon_t \times \mathrm{l_e})/(\mathrm{f_t} \times \mathrm{l_e}) \quad (5)$$

where f_t = Uniaxial tensile strength. The compressive behaviour of this model uses non-linear hardening plasticity theory with a yield criterion that is obtained by fitting biaxial experimental results.

2.1 Yield Criterion

In this paper, a yield criterion proposed by Owen et al. [13] was employed. This criterion is formulated in terms of the first two stress invariants and only two material parameters are involved in its definition.

$$F(I_1, J_2) = \left[\beta(3J_2) + \alpha I_1\right]^{1/2} = \bar{\sigma} \tag{6}$$

where α and β are material parameters and $\bar{\sigma}$ is the effective stress (or equivalent yield stress) taken as the compressive stress from a uniaxial test. $I_1 = \sigma_1 + \sigma_2 + \sigma_3$, and

$$J_2 = \frac{1}{6}\left[(\sigma_1 - \sigma_2)^2 + (\sigma_2 - \sigma_3)^2 + (\sigma_3 - \sigma_1)^2\right]$$

In terms of principal stresses, the expression for yielding can be written as,

$$\beta\left[\frac{1}{2}\left[(\sigma_1 - \sigma_2)^2 + (\sigma_2 - \sigma_3)^2 + (\sigma_3 - \sigma_1)^2\right]\right] + \alpha(\sigma_1 + \sigma_2 + \sigma_3) = \bar{\sigma}^2 \tag{7}$$

where σ_1, σ_2, and σ_3 are the principal stresses referring to the principal stress axes, 1, 2, and 3.

To fit the data of Kuper et. al [14], the parameters take the values:

$\alpha = 0.355\ \bar{\sigma}$, $\beta = 1.355$

Substituting the above two values into (7) and rearranging gives

$$\bar{\sigma} = CI_1 + \sqrt{C^2 I_1^2 + DJ_2} = 0 \tag{8}$$

Or $\bar{\sigma}$ = $F(I_1,J_2)$ in which C = 0.1775, D = 4.065; $\bar{\sigma}$ = equivalent yield stress; $F(I_1,J_2)$ is yield surface.

2.2 Flow Rule

The flow rule is assumed to be associated to the compressive yield surface. The gradient of the yield surface is given by :

$$\frac{\partial F}{\partial \sigma_{ij}} = \frac{\partial \mathrm{F}}{\partial \mathrm{I}_1}\frac{\partial \mathrm{I}_1}{\partial \sigma_{ij}} + \frac{\partial \mathrm{F}}{\partial \mathrm{J}_2}\frac{\partial \mathrm{J}_2}{\partial \sigma_{ij}} \tag{9}$$

where

$$\frac{\partial \mathrm{F}}{\partial \mathrm{I}_1} = C + \frac{C^2 I_1}{\sqrt{C^2 I_1^2 + DJ_2}} \tag{10}$$

$$\frac{\partial \mathrm{F}}{\partial \mathrm{J}_2} = C + \frac{D}{2\sqrt{C^2 I_1^2 + DJ_2}} \tag{11}$$

$$\frac{\partial \mathrm{I}_1}{\partial \sigma_{ij}} = \delta_{ij} \tag{12}$$

2. 3 Hardening Rule

The hardening rule adopted in concrete is usually obtained by fitting the experimental data. In this study, the hardening rule proposed by Jefferson and Wright [4]. The hardening parameter is obtained from Saenz's equation [15].

Saenz's equation can be expressed as：

$$\bar{\sigma} = \frac{E_0 \varepsilon_u}{1 + \left[\frac{E_0}{E_s} - 2\right]\frac{\varepsilon_u}{\varepsilon_c'} + \left(\frac{\varepsilon_u}{\varepsilon_c'}\right)^2} \tag{13}$$

where E_o = initial Young's modulus, ε_u = uniaxial strain, ε_c' = uniaxial strain at peak stress, σ_c = peak uniaxial stress.

$$E_s = \frac{\sigma_c'}{\varepsilon_c'}$$

From the definition of H (Hardening parameter), the following equation can be obtained:

$$H = \frac{d\sigma}{d\varepsilon_p} = \frac{d\sigma}{d\varepsilon - d\varepsilon_e} = \frac{1}{\frac{d\varepsilon}{d\sigma} - \frac{d\varepsilon_e}{d\sigma}} = \frac{\frac{d\sigma}{d\varepsilon}}{1 - \frac{d\sigma}{d\varepsilon}\frac{d\varepsilon_e}{d\sigma}} = \frac{E_T}{1 - E_T / E_o} \tag{14}$$

where σ = stress, ε = strain, ε_p = plastic strain, ε_e =elastic strain.

$$E_T = \frac{d\sigma}{d\varepsilon}$$

2.4 Simple dilatancy law

The dilatancy effect in the open crack state (Fig. 3), i.e. when a crack is fully opened, has been evaluated by fitting experimental data [7-9,11] and the detailed findings will be introduced in the next section.

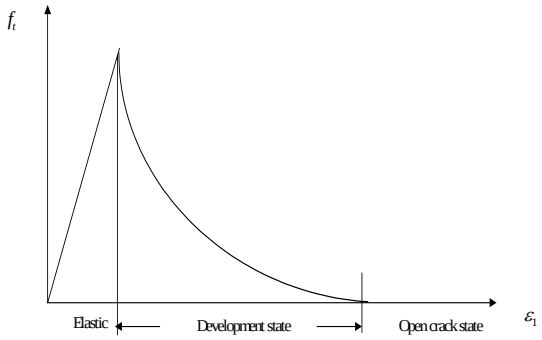

Fig. 3. Three states in the cracking process.
Where ε_1 is the tensile strain and f_t is the tensile stress

However, since the dilatancy effect cannot be isolated from other effects in the experimental result, the empirical formula (stress-strain relationship) cannot be derived directly for the crack development state. In this study it is proposed that by increasing the shear slip, a certain amount of volumetric increase will be caused. This leads to either free expansion or an increase in the compressive stress if confined. Consequently, the dilatancy effect could be simulated by considering the amount of volumetric change or the change in compressive stress in confined conditions.

In concrete, unlike in a soil structure, the dilatancy effect is confined to the crack surface and the uncracked area is usually regarded to exhibit very little dilatancy effect. Hence, in the application to concrete structures, the volumetric changes can usually be simplified as a change in the normal strain. Therefore, the dilatancy effect in a concrete structure usually can be modelled as the coupling between normal and shear strain [7,11].

On the basis of the above assumption, a simple dilatancy criterion was proposed in this study to model the dilatancy effect.

The fundamental feature of this simple dilatancy model proposed in this study is a decomposition of the total strain increment $\Delta\varepsilon$ into a non-dilative concrete strain increment $\Delta\varepsilon^N$ and a dilative normal strain increment $\Delta\varepsilon^D$:

In a two dimensional case, they may be represented as follows, in the direction of crack.

$$\Delta\varepsilon_{11} = \Delta\varepsilon_{11}^N + \Delta\varepsilon_{11}^D \tag{15}$$

$$\Delta\varepsilon_{22} = \Delta\varepsilon_{22}^N + \Delta\varepsilon_{22}^D \tag{16}$$

while the shear strain is not affected.

In a three dimensional case, if the change of volume is represented as $\Delta\Omega$ and per unit volume of the material is represented as Ω, the volumetric dilatation is related to the normal strains as follows:

$$\frac{\Delta\Omega}{\Omega} = \Delta\varepsilon_{11} + \Delta\varepsilon_{22} + \Delta\varepsilon_{33} \tag{17}$$

and the dilatancy law is represented as

$$\frac{\Delta\varepsilon_{11}^D + \Delta\varepsilon_{22}^D + \Delta\varepsilon_{33}^D}{|\Delta\gamma_{12}|} = \mu \tag{18}$$

where $\Delta\varepsilon_{11}^D$ = Concrete strain increment in 1 direction i.e. normal to the crack plane. $\Delta\varepsilon_{22}^D$ = Concrete strain increment in 2 direction i.e. perpendicular to 1 direction. $\Delta\varepsilon_{33}^D$ = Concrete strain increment in 3 direction i.e. perpendicular to 1 and 2 directions. $\Delta\gamma_{12}$ = Concrete shear strain increment.

To consider the crack dilatancy effect in both plane stress and plane strain cases, since this effect is produced on the crack surface and the uncracked area is usually regarded to exhibit very little dilatancy effect, if the cracks are only allowed to form in the 1 and 2 directions, the non-cracked direction would exhibit only very little dilatancy effect and can be ignored, i.e. $\Delta\varepsilon_{33}^D = 0$.

Therefore, in the plane stress and plane strain problems, the dilatancy law can be represented as:

$$\frac{\Delta\varepsilon_{11}^D + \Delta\varepsilon_{22}^D}{|\Delta\gamma_{12}|} = \mu \tag{19}$$

$$\Delta\varepsilon_{11}^D + \Delta\varepsilon_{22}^D = \mu|\Delta\gamma_{12}| \tag{20}$$

where μ is defined as a constant dilatancy parameter and the value is presented as:

$\mu = \mu_1$ for the crack development state
$\mu = \mu_2 = 1$ for the open crack state

Three stages in the cracking process can be distinguished: (1) The linear-elastic state; (2) the

development state; and (3) the open-crack, as shown in Fig. 3. In the crack development state, as there is no experimental evidence, the value of dilatancy parameter cannot be estimated from the experiment. Therefore, a number of values will be investigated to explore the influence in the latter sections. In the open crack state, the value of the dilatancy parameter has been estimated to be 1 obtained by fitting the experimental results and more details will be presented in next section.

In Eqs. 19 and 20 the absolute value of incremental shear strain $\Delta\gamma_{12}$ is adopted; this implies that no matter in which direction the incremental shear strain $\Delta\gamma_{12}$ is, the incremental dilatancy term will always give a positive value i.e. expansion. This is correct if the incremental shear strain $\Delta\gamma_{12}$ is in the same direction as the current shear strain γ_{12}, i.e. loading. In conditions of unloading, i.e. $\Delta\gamma_{12}$ is in the opposite direction to shear strain γ_{12}, the dilatancy law can be represented as:

$$\Delta\varepsilon_{11}^{D} + \Delta\varepsilon_{22}^{D} = -\mu\left|\Delta\gamma_{12}\right| \tag{21}$$

This implies that the incremental dilatancy term will give a negative value, i.e. reduction in the volumetric strain. Although the incremental dilatancy term may give a positive or negative value in different conditions, the total dilatancy term will always give a positive value. In concrete, the dilatancy will lead to an increase in volume, and consequently the total dilatancy term always has a positive value.

In order to satisfy the demands in both loading and unloading conditions, the dilatancy law can be represented as:

$$\Delta\varepsilon_{11}^{D} + \Delta\varepsilon_{22}^{D} = \mu\frac{\gamma_{12}}{\left|\gamma_{12}\right|}\Delta\gamma_{12} \tag{22}$$

We further define a second parameter k_1, relating to the distribution of volumetric changes in the two principal directions, such that

$$k_1 = \frac{\Delta\varepsilon_{11}^{D}}{\Delta\varepsilon_{11}^{D} + \Delta\varepsilon_{22}^{D}} \tag{23}$$

Following Eq.18 and 19 we can derive that:

$$\Delta\varepsilon_{11}^{D} = k_1\mu\frac{\gamma_{12}}{\left|\gamma_{12}\right|}\Delta\gamma \quad \text{and}$$

$$\Delta\varepsilon_{22}^{D} = (1-k_1)\mu\frac{\gamma_{12}}{\left|\gamma_{12}\right|}\Delta\gamma \tag{24}$$

After the dilative strain increment $(\Delta\varepsilon^{D})$ is obtained, the next step is to consider the following cases.

Case I: Free expansion (see Figs. 4 and 5).

Case II: Confined by boundary restrain (see Fig. 6).

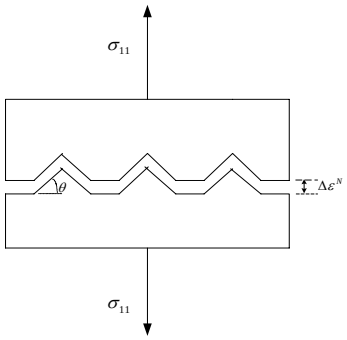

Fig. 4. A specimen subject to pure tensile force

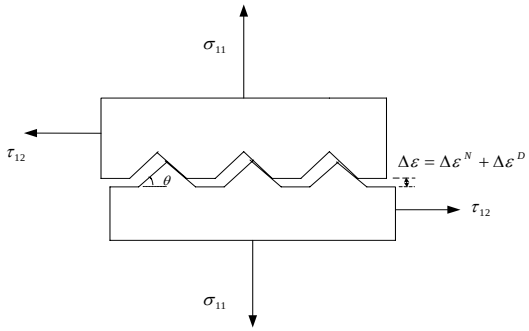

Fig. 5. A specimen subject to tensile and shear forces simultaneously Case I: Free expansion

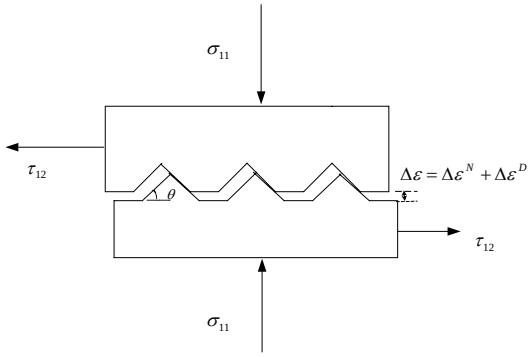

Fig. 6. A specimen subject to compressive and shear forces simultaneously Case II: Confined by boundary restrain

Case I: Free expansion

In this case, there is no compressive stress developed on the crack surface. The influence of the dilatancy effect can be evaluated indirectly by adopting the non-dilative tensile concrete strain ε^N to fit the strain softening curve (Fig. 1) rather than total tensile strain.

Since the strain softening curve (Fig. 1) or most other softening curves were obtained by fitting pure tension test or simulated pure tension test data, i.e. shear stress is assumed to be zero or very small value, consequently, the softening curve should have the best performance when applied to a specimen subjected to pure tension. However, when applied to a specimen subjected to tension and shear forces simultaneously, this curve may not be very correct.

Assuming that a strain softening curve (Fig. 7), we further assume that another strain softening curve has been obtained by fitting a test that is subjected to tensile and shear forces simultaneously. Since there is no experimental evidence available, a strain softening curve (dash line) is assumed and shown in Fig. 8. In order to obtain the tensile stress, one should use the total tensile strain (ε) to fit the softening curve under both tensile and shear conditions. However, due to the lack of experimental data, the softening curve under both tensile and shear condition is not available. An alternative presented in this study is to adopt the non-dilative tensile strain (ε^N) to fit the softening curve obtained from the tensile effect only as shown in Fig. 7.

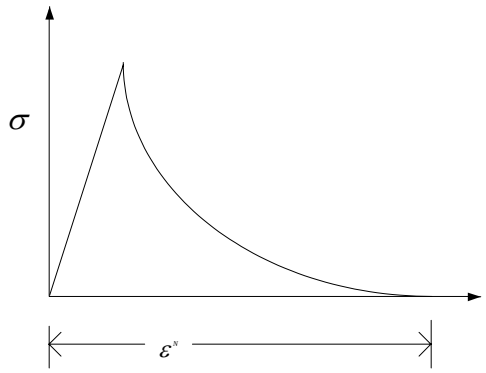

Fig. 7. Strain softening curve.

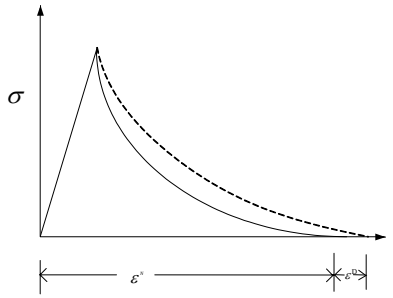

Fig. 8. Assumed strain softening curve.

For the formation of the global stiffness matrix, the non-dilative cracked tangential D-matrix (Eq. 1) needs to be converted into the dilative crack including tangential D-matrix. Substituting Eq. 24 into Eq.1 the following equation can be derived:

For loading i.e. $\frac{\gamma_{12}}{|\gamma_{12}|}=1$

$$\begin{bmatrix}\Delta\varepsilon_{11}\\ \Delta\varepsilon_{22}\\ \Delta\gamma_{12}\end{bmatrix}=\begin{bmatrix}\Delta\varepsilon_{11}^N+\Delta\varepsilon_{11}^D\\ \Delta\varepsilon_{22}^N+\Delta\varepsilon_{22}^D\\ \Delta\gamma_{12}\end{bmatrix}$$

$$=\begin{bmatrix}1/D_1(\varepsilon_{11}) & 0 & k_1\mu/\beta G\\ 0 & 1/D_2(\varepsilon_{22}) & (1-k_1)\mu/\beta G\\ 0 & 0 & 1/\beta G\end{bmatrix}\begin{bmatrix}\Delta\sigma_{11}\\ \Delta\sigma_{22}\\ \Delta\tau_{12}\end{bmatrix} \quad (25)$$

Then the cracked tangential D-matrix for a single crack, by inverting Eq. 25 will be

$$\mathrm{D}_{\mathrm{cr}}=\begin{bmatrix}D_1(\varepsilon_{11}) & 0 & -D_1\mu k_1\\ 0 & D_2(\varepsilon_{22}) & -D_2\mu(1-k_1)\\ 0 & 0 & \beta G\end{bmatrix} \quad (26)$$

For unloading 1.e. $\frac{\gamma_{12}}{|\gamma_{12}|}=-1$

$$\begin{bmatrix}\Delta\varepsilon_{11}\\ \Delta\varepsilon_{22}\\ \Delta\gamma_{12}\end{bmatrix}=\begin{bmatrix}\Delta\varepsilon_{11}^N+\Delta\varepsilon_{11}^D\\ \Delta\varepsilon_{22}^N+\Delta\varepsilon_{22}^D\\ \Delta\gamma_{12}\end{bmatrix}$$

$$=\begin{bmatrix}1/D_1(\varepsilon_{11}) & 0 & -k_1\mu/\beta G\\ 0 & 1/D_2(\varepsilon_{22}) & -(1-k_1)\mu/\beta G\\ 0 & 0 & 1/\beta G\end{bmatrix}\begin{bmatrix}\Delta\sigma_{11}\\ \Delta\sigma_{22}\\ \Delta\tau_{12}\end{bmatrix} \quad (27)$$

$$\mathrm{D}_{\mathrm{cr}} = \begin{bmatrix} D_1(\varepsilon_{11}) & 0 & D_1\mu k_1 \\ 0 & D_2(\varepsilon_{22}) & D_2\mu(1-k_1) \\ 0 & 0 & \beta G \end{bmatrix} \quad (28)$$

Comparing Eqs. 1, 26 and 28, it can be seen that some of the non-diagonal terms are now non-zero; this implies that the dilatancy effect has induced coupling between normal stress and shear stress. From Eq. 1, the incremental normal strain can be calculated as

$$\Delta\varepsilon_{11} = \frac{1}{D_1(\varepsilon_{11})}\Delta\sigma_{11} \quad (29)$$

$$\Delta\varepsilon_{22} = \frac{1}{D_2(\varepsilon_{22})}\Delta\sigma_{22} \quad (30)$$

However, from Eq. 25 (assuming that $\frac{\gamma_{12}}{|\gamma_{12}|} = 1$), the incremental normal strain in 1-direction can now be derived as

$$\Delta\varepsilon_{11} = \frac{1}{D_1(\varepsilon_{11})}\Delta\sigma_{11} + \frac{k_1\mu}{\beta G}\Delta\tau_{12} \quad (31)$$

$$\Delta\varepsilon_{22} = \frac{1}{D_2(\varepsilon_{22})}\Delta\sigma_{22} + \frac{(1-k_1)\mu}{\beta G}\Delta\tau_{12} \quad (32)$$

Comparing Eqs. 29, 30, 31 and 32, it can be seen that the shear stress in the non-dilating fixed crack approach produces no normal strain. This implies that the shear slip on crack surfaces can occur at constant crack opening and this is obviously not true due to the aggregate interlock [7-9,11].

In contrast, the simple dilatancy approach allows a certain amount of normal strain that is proportional to the shear strain to be produced (Eq. 24). This implies that an increase of shear slip will produce an increase of crack opening and this is in accordance with experimental observation.

Case II: Confined by boundary restrain

According to the dilatancy experiments completed by Paulay and Loeber [7]; Bazant and Gambarova [11], Walraven and Reinhardt [8], and Gambarova and Karakoc [9], as stated in the previous section, “A shear slip on crack surfaces cannot occur at constant crack opening displacement. Furthermore, if the opening is restrained then a large compressive stress is introduced on the crack surface”. An approach that allows an increase of shear slip to produce an increase of crack opening has been presented in the previous case (Case I). In this case, another approach is developed to model the case that the crack opening is restrained and a large compressive stress is introduced on the crack surface.

In this case, since the crack opening is restrained, a compressive stress on the crack surface will occur. In order to properly evaluate the magnitude of the compressive stress, the elasto-plastic theory must be adopted. The following steps need to be employed when the compressive yield surface is reached.

At some stage after initial yielding, consider a further load application resulting in an incremental increase of stress, $\Delta\sigma$, accompanied by a change of non-dilative strain, $\Delta\varepsilon^N$. In this study, it is assumed that the strain can be separated into elastic and plastic components, so that

$$\Delta\varepsilon^N = \Delta\varepsilon^e + \Delta\varepsilon^p \quad (33)$$

where $\Delta\varepsilon^e$ = Elastic strain increment, $\Delta\varepsilon^p$ = Plastic strain increment. Therefore, the total concrete strain increment $\Delta\varepsilon$ can be represented as

$$\Delta\varepsilon = \Delta\varepsilon^N + \Delta\varepsilon^D = \Delta\varepsilon^e + \Delta\varepsilon^p + \Delta\varepsilon^D \quad (34)$$

where $\Delta\varepsilon^N$ = Non-dilative concrete strain increment, $\Delta\varepsilon^D$ = Dilative normal strain increment, $\Delta\varepsilon^e$ = Elastic strain increment.

(1) Elastic stress-strain relationships

$$\Delta\sigma = D_e\,\Delta\varepsilon^e \quad (35)$$

where D_e is the elastic stress-strain matrix.

(2) Flow rule

$$\Delta\varepsilon^p = \Delta\lambda\,\frac{\partial \mathrm{Q}}{\partial\sigma} \quad (36)$$

where Q = Plastic potential function, $\Delta\lambda$ =

The plastic multiplier, $\Delta\varepsilon_p$ = Equivalent uniaxial plastic strain increment.

If the flow potential function is equal to the yield function (F), then the flow is said to be 'associated' and the plastic strain is then given by:

$$\Delta\varepsilon^p = \Delta\lambda \frac{\partial \mathrm{F}}{\partial \sigma} \tag{37}$$

(3) Hardening relationship

$$A\Delta\lambda = \left(\frac{\partial \mathrm{F}}{\partial \sigma}\right)^T \Delta\sigma \tag{38}$$

Using equation (34) and (35) then the following can be obtained

$$\begin{aligned}\Delta\sigma &= D_e\,\Delta\varepsilon^{\,e} = D_e(\Delta\varepsilon - \Delta\varepsilon^{\,p} - \Delta\varepsilon^{\,D}) \\ &= D_e(\Delta\varepsilon^N - \Delta\varepsilon^{\,p})\end{aligned} \tag{39}$$

Therefore, Eq. 39 can be represented as

$$\Delta\sigma = D_{\mathrm{e}}(\Delta\varepsilon^N - \Delta\lambda \frac{\partial \mathrm{F}}{\partial \sigma}) \tag{40}$$

Rearranging (Eq. 40) and premultiplying by $(\frac{\partial \mathrm{F}}{\partial \sigma})^T$ gives:

$$(\frac{\partial \mathrm{F}}{\partial \sigma})^T \Delta\sigma = (\frac{\partial \mathrm{F}}{\partial \sigma})^T \mathrm{D_e}(\Delta\varepsilon^N - \Delta\lambda \frac{\partial \mathrm{F}}{\partial \sigma}) \tag{41}$$

By substituting Eq. 38 into Eq. 41, the following can be obtained

$$A\Delta\lambda = (\frac{\partial \mathrm{F}}{\partial \sigma})^T \mathrm{D_e}(\Delta\varepsilon^N - \Delta\lambda \frac{\partial \mathrm{F}}{\partial \sigma}) \tag{42}$$

Rearranging Eq. 42 will give:

$$\Delta\lambda[\mathrm{A} + (\frac{\partial \mathrm{F}}{\partial \sigma})^T \mathrm{D_e} \frac{\partial \mathrm{F}}{\partial \sigma}] = (\frac{\partial \mathrm{F}}{\partial \sigma})^T \mathrm{D_e}\,\Delta\varepsilon^N \tag{43}$$

Therefore, the plastic multiplier $\Delta\lambda$ can be represented as

$$\Delta\lambda = \frac{(\frac{\partial \mathrm{F}}{\partial \sigma})^T \mathrm{D_e}\,\Delta\varepsilon^N}{[\mathrm{A} + (\frac{\partial \mathrm{F}}{\partial \sigma})^T \mathrm{D_e} \frac{\partial \mathrm{F}}{\partial \sigma}]} \tag{44}$$

By substituting (44) into (40) and the elasto-plastic-dilatancy relationship can be obtained as follows:

$$\Delta\sigma = D_{\mathrm{e}}(\Delta\varepsilon^N - \frac{(\frac{\partial \mathrm{F}}{\partial \sigma})^T \mathrm{D_e}\,\Delta\varepsilon^N}{[\mathrm{A} + (\frac{\partial \mathrm{F}}{\partial \sigma})^T \mathrm{D_e} \frac{\partial \mathrm{F}}{\partial \sigma}]} \frac{\partial \mathrm{F}}{\partial \sigma}) \tag{45}$$

$$= (D_{\mathrm{e}} - \frac{D_{\mathrm{e}} \frac{\partial \mathrm{F}}{\partial \sigma} (\frac{\partial \mathrm{F}}{\partial \sigma})^T \mathrm{D_e}}{[\mathrm{A} + (\frac{\partial \mathrm{F}}{\partial \sigma})^T \mathrm{D_e} \frac{\partial \mathrm{F}}{\partial \sigma}]})\Delta\varepsilon^N \tag{46}$$

$$= D_{ep}\Delta\varepsilon^N \tag{47}$$

where

$$D_{ep} = D_{\mathrm{e}} - \frac{D_{\mathrm{e}} \frac{\partial \mathrm{F}}{\partial \sigma} (\frac{\partial \mathrm{F}}{\partial \sigma})^T \mathrm{D_e}}{[\mathrm{A} + (\frac{\partial \mathrm{F}}{\partial \sigma})^T \mathrm{D_e} \frac{\partial \mathrm{F}}{\partial \sigma}]} \tag{48}$$

2.5 Forming the full D matrix D_{epd}

In order to form the full D matrix, the equation (Eq. 47) needs to be represented by $\Delta\varepsilon$ rather than $\Delta\varepsilon^N$. Substituting equation (Eq. 34) into equation (Eq. 47), the following equation is given.

$$\Delta\sigma = D_{ep}\Delta\varepsilon^N = D_{ep}(\Delta\varepsilon - \Delta\varepsilon^D) \tag{49}$$

Recalling that

$$\Delta\varepsilon_{11}^D + \Delta\varepsilon_{22}^D = \mu\frac{\gamma_{12}}{|\gamma_{12}|}\Delta\gamma_{12} \tag{50}$$

Therefore, $\Delta\varepsilon_{11}^D = k_1\mu\Delta\gamma_{12}\frac{\gamma_{12}}{|\gamma_{12}|}$ and

$$\Delta\varepsilon_{22}^D = (1-k_1)\mu\Delta\gamma_{12}\frac{\gamma_{12}}{|\gamma_{12}|} \tag{51}$$

$$\text{Set} \quad D_n = \frac{\gamma_{12}}{|\gamma_{12}|}\begin{bmatrix} 0 & 0 & k_1\mu \\ 0 & 0 & (1-k_1)\mu \\ 0 & 0 & 0 \end{bmatrix} \tag{52}$$

Therefore, equation (47) can be rearranged as

$$\begin{aligned} \Delta\sigma &= D_{ep}\Delta\varepsilon^N \\ &= D_{ep}(\Delta\varepsilon - \Delta\varepsilon^D) \\ &= D_{ep}\{[I] - D_n\}\Delta\varepsilon \\ &= \mathrm{D}_{\mathrm{epd}}\Delta\varepsilon \end{aligned} \tag{53}$$

where $D_{ep}\{[I]-D_n\} = \mathrm{D}_{\mathrm{epd}}$, which is the full D matrix for dilatancy effect with compression failure.

2.6 Estimating the dilatancy parameter μ from the experiments

In order to estimate the range of value of the dilatancy parameter μ in the open crack state, the experimental diagrams available in the open crack state are used for this task.

The experimental diagrams collected in this study include Aggregate-Interlock Relation [8], Rough Crack Model [11] and Rough Crack Model [9], as shown in Figs. 9, 10 and 11. In these diagrams, f_1 is the confinement normal stress and u_1 and u_2 are the normal and shear displacements. The relations are shown as follows:

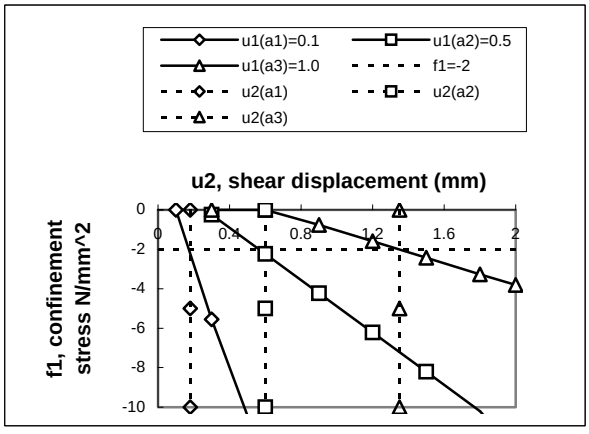

Fig. 9. Response diagram of Aggregate-Interlock Relation (Walraven and Reinhardt 1981)

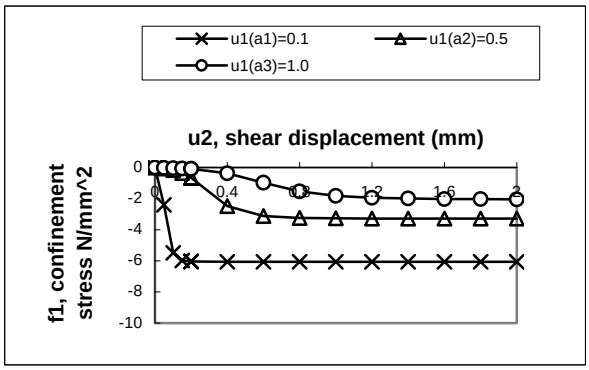

Fig. 10. Response diagram of Rough Crack Model (Bazant and Gambarova 1980)

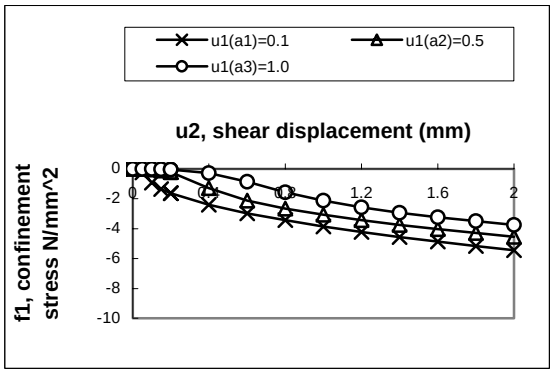

Fig. 11. Response diagram of Rough Crack Model (Gambarova and Karakoc 1983)

2.6.1 Aggregate-Interlock Relation (Walraven and Reinhardt (1981))

The response diagram of this model is shown in Fig. 9. The confinement normal stress f_1 (N/mm^2) and shear stress f_2 (N/mm^2) are shown as follows:

$$f_1 = \frac{f_{cc}}{20} - [1.35\Delta u_1^{-0.63} + (0.191\Delta u_1^{-0.552} - 0.15) f_{cc}]\Delta u_2 \tag{54}$$

$$f_2 = \frac{f_{cc}}{30} + [1.8\Delta u_1^{-0.80} + (0.234\Delta u_1^{-0.707} - 0.20) f_{cc}]\Delta u_2 \tag{55}$$

where Δu_1 = Normal displacement (mm), Δu_2 = Shear displacement (mm), f_{cc} =Compressive cube strength.

2.6.2 Rough Crack Model (Bazant and Gambarova (1980))

The response diagram of this model is shown in Fig. 10. The confinement normal stress f_1

(N/mm^2) and shear stress f_2 (N/mm^2) are shown as follows:

$$f_1 = -\frac{a_1}{\Delta u_1}(a_2|f_2|)^p \quad (56)$$

$$f_2 = \tau_u r \frac{a_3 + a_4|r|^3}{1 + a_4 r^4} \quad (57)$$

where $p = 1.3 \times [1 - 0.231/(1 + 0.185\Delta u_1 + 0.563\Delta u_1^{\ 2})]$, $r = \Delta u_2 / \Delta u_1$, $\tau_u = \tau_0 a_0 / [a_0 + (\Delta u_1)^2]$, $a_0 = 0.01 D_{\max}^2$, $a_1 = 0.000534$, $a_2 = 145.0$, $a_3 = 2{,}45/\tau_0$, $a_4 = 2.44(1 - 4/\tau_0)$; and $\tau_0 = 0.245 f_c = 0.195 f_{cc}$, $r = \Delta u_2 / \Delta u_1$, Δu_1 = normal displacement, Δu_2 = shear displacement.

The notation f_c is used for the compressive cylinder strength of the concrete, and the more frequently used compressive cube strength is denoted by f_{cc}.

2.6.3 Rough Crack Model (Gambarova and Karakoc (1983))

The response diagram of this model is shown in Fig. 11. The confinement normal stress f_1 (N/mm^2) and shear stress f_2 (N/mm^2) are shown as follows:

$$f_1 = -a_1 a_2 \sqrt{\Delta u_1}\ \frac{r}{\left(1 + r^2\right)^{0.25}}\ \cdot f_2 \quad (58)$$

$$f_2 = \tau_0 \left(1 - \sqrt{\frac{2\Delta u_1}{D_{\max}}}\right) r \frac{a_3 + a_4|r|^3}{1 + a_4 r^4} \quad (59)$$

where $a_1 a_2 = 0.62$, $a_3 = 2.45/\tau_0$, $a_4 = 2.44(1 - 4/\tau_0)$; and $\tau_0 = 0.25 f_c = 0.2 f_{cc}$, $r = \Delta u_2 / \Delta u_1$, Δu_1 = Normal displacement (mm), Δu_2 = Shear displacement (mm), D_{max} = The maximum aggregate size (mm).

The dilatancy parameter μ can be obtained using Eq.19. In addition, since the dilatancy tests were conducted on the basis of a single crack only (assuming ε_{22}=0), Eq.19 can be simplified as:

$$\frac{\Delta \varepsilon_{11}^D}{\Delta \gamma_{12}} = \mu \quad (60)$$

In a single crack, the dilatancy parameter is assumed to be constant. But the most appropriate value of μ should be the one derived with zero confining normal stress. However, as the experiment was performed under constant separation condition, some manipulations are needed to obtain the value of the dilatancy parameter. In these manipulations, we simply assume that the parameters are not strongly affected by the stress path.

Starting from a given point on the experimental curve with normal stress (f_1(a)) & shear stress (f_2(a)), normal displacement (u_1(a)) & shear displacement (u_2(a)), the test proceeds to the next state of normal stress (f_1(b)) & shear stress (f_2(b)) and (u_1(a)) & (u_2(b)) with u_1(a) remaining unchanged. In this case, the volumetric change has been suppressed by the increase in normal stress. If the normal stress kept constant, the normal displacement would need to increase with increasing shear displacement. By considering values of normal displacement for a constant confined stress, we assume that the increase in normal displacement between different experimental curves is equal to the volumetric expansion required to keep the normal stress constant when the shear deformation is increased. Values of the dilatancy parameter can then be obtained by considering the incremental normal and shear displacement.

For

$$\mu = \frac{\Delta \varepsilon_{11}^D}{\Delta \gamma_{12}} = \frac{\text{incremental normal displacements}}{\text{incremental shear displacements}} \quad (61)$$

Using the experimental diagram used in the Aggregate-Interlock Relation [8], and finding a set of values of u_2(a1), u_2(a2), u_1(a1), and u_1(a2) and another set of values of u_2(a2), u_2(a3), u_1(a2), and u_1(a3) from Fig.9, the dilatancy parameter can then be estimated using

$$\mu(1) = \frac{\Delta \varepsilon_{11}^D}{\Delta \gamma_{12}} = \frac{u_1(a2) - u_1(a1)}{u_2(a2) - u_2(a1)} = \frac{0.5 - 0.1}{u_2(a2) - u_2(a1)} \quad (62)$$

$$\mu(2) = \frac{\Delta\varepsilon_{11}^{D}}{\Delta\gamma_{12}} = \frac{u_1(a3) - u_1(a2)}{u_2(a3) - u_2(a2)} = \frac{1.0 - 0.5}{u_2(a3) - u_2(a2)} \quad (63)$$

Where a1, a2 and a3 are used to distinguish different values of u1 and u2; $\mu(1)$ and $\mu(2)$ represent two sets of dilatancy parameters.

Repeating the process, a number of estimates for the dilatancy parameter μ can be obtained from the experimental diagram, as shown in Figs. 12, 13 and 14. It can be seen that the range of the dilatancy parameter μ is between 1.6 ~ 0.2 for experimental data from Aggregate-Interlock Relation [8]. The range of the dilatancy parameter μ is between 4.0 ~ 0.5 for Rough Crack Model [11] and is between 3.0 ~ 0.8 for Rough Crack Model [9]. In addition, it can be seen that all these diagrams show that the dilatancy parameter μ decreases with the increasing confinement stress. This is consistent with the fact that the crack opening displacement decreases with the increasing confinement stress.

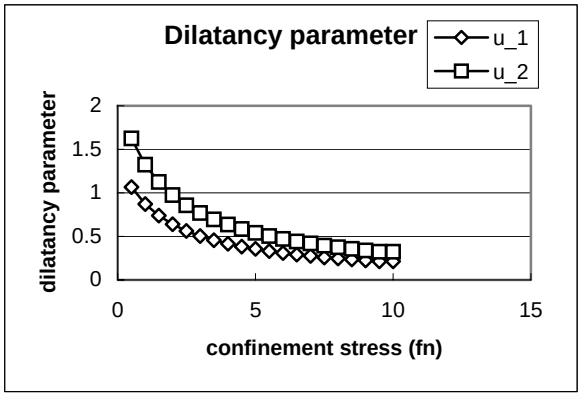

Fig. 12. Dilatancy parameters obtained by fitting the Aggregate-Interlock Relation (1981). (The symbols u_1 and u_2 represents the dilatancy parameters $\mu(1)$ and $\mu(2)$ respectively.)

It can be safely assumed that the value of dilatancy parameter would be a function of the size and shape of the aggregate. However, the shapes of the aggregate have not been reported with the experimental results. In this study, a value of the dilatancy parameter μ for zero confined stress has been taken as 1.0 after considering that the sloping angle of the shape of the aggregate can be reasonably taken as 45°.

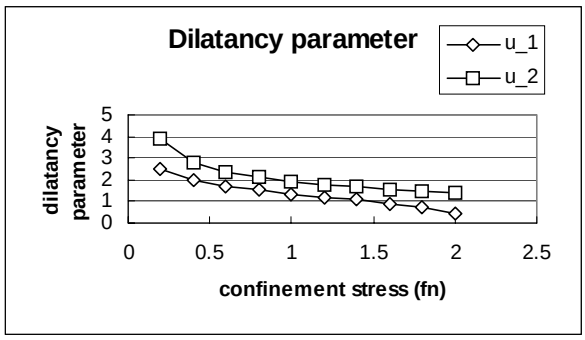

Fig. 13. Dilatancy parameter obtained by fitting the Rough Crack Model (1980) (The symbols u_1 and u_2 represents the dilatancy parameters $\mu(1)$ and $\mu(2)$ respectively.)

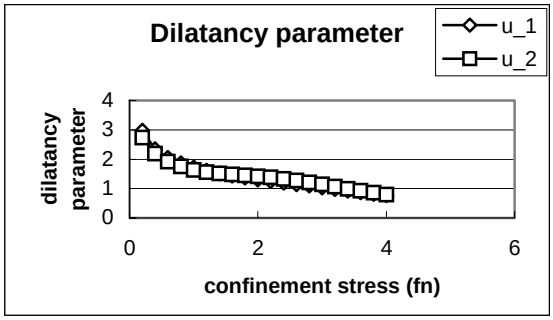

Fig. 14. Dilatancy parameter obtained by fitting the Rough Crack Model (1983) (The symbols u_1 and u_2 represent the dilatancy parameter $\mu(1)$ and $\mu(2)$ respectively.)

III. SINGLE ELEMENT TEST

3.1 Single element test (I)

The single element test used is adopted to examine the accuracy of the Finite Element implementation in the LUSAS MMI [16].

The dimensions of the cubic element used in this example are again 50mm*50mm, and the thickness is 50mm. In this analysis, 1 element with 9 Gauss points is adopted and the displacements of all the nodes are prescribed.

The accuracy of the implementation of the proposed crack model is examined using two loading paths. For the first loading path, the element is made to perform tensile behavior first and then compressive behavior and finally tensile behavior. For the second loading path, the element is made to perform compressive behavior first and then tensile behavior and finally compressive

behavior.

The results of this numerical test of the proposed crack model are shown from Figs. 15 to 16. By comparing these curves with that presented in previous section, it can be seen that the implementation of this model have been successful.

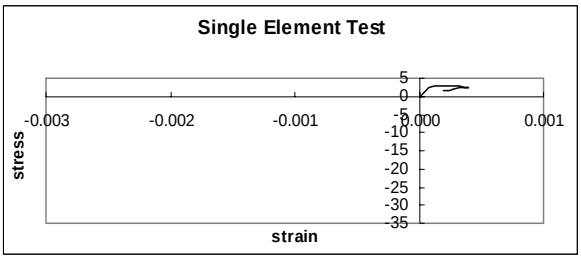

Step 1: Tension

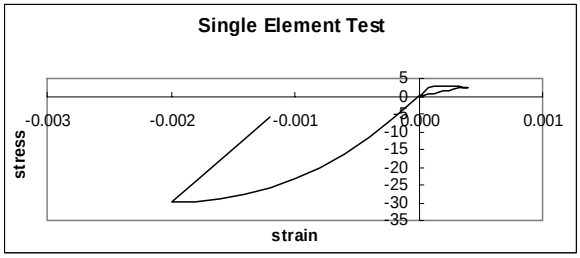

Step 2: Compression

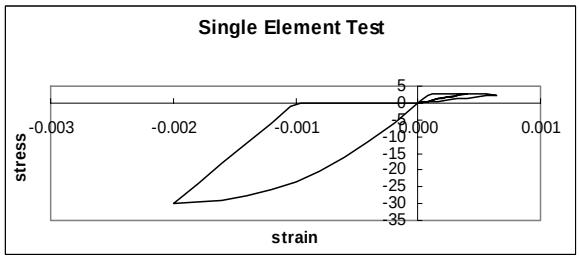

Step 3: Tension

Fig. 15. Single element test
(tension-> compression->tension)

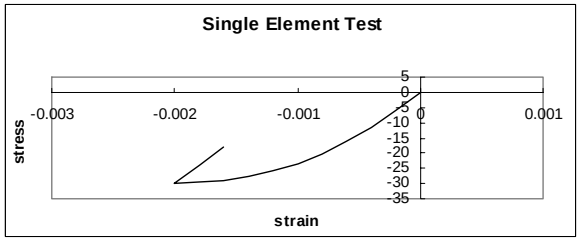

Step 1: Compression

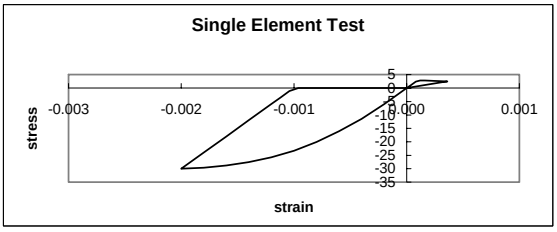

Step 2: Tension

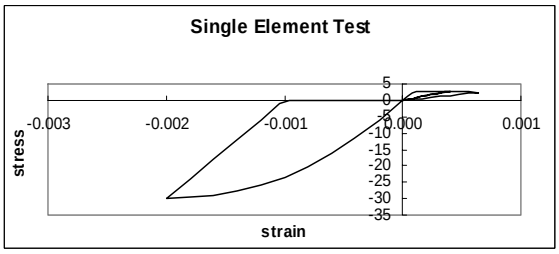

Step 3: Compression

Fig. 16. Single element test
(compression->tension-> compression)

3.2 Single element test (II)

Again, the single element tests with displacement control were carried out to validate the implementation of the dilatancy law.

Initially, we control in the first step so that the boundary conditions in the 1 and 2 directions become $\frac{\Delta\varepsilon_{22}}{\Delta\varepsilon_{11}} = -\nu ; \Delta\gamma_{12} = 0$ in the linear elastic state until a crack appears. After the concrete has cracked, a switch is made and the shear strain is applied in the y direction. In the current analysis, the number of total displacement increments is chosen as 10. Observing the output result, it is found that the concrete cracked in the sixth displacement increment. Therefore, the second displacement control is applied from the seventh displacement increment onward.

Furthermore, the dilatancy parameter μ_1 is varied from 0.0 to 0.4 and the ratio of the shear strain over normal strain was chosen as 1.0 and 2.0, i.e. $\frac{\Delta\gamma_{12}}{\Delta\varepsilon_{11}} = 1.0$ and $\frac{\Delta\gamma_{12}}{\Delta\varepsilon_{11}} = 2.0$.

The results for the simple dilatancy criterion for $\frac{\Delta\gamma_{12}}{\Delta\varepsilon_{11}} = 1.0$ are shown in Fig. 17 and the result for $\frac{\Delta\gamma_{12}}{\Delta\varepsilon_{11}} = 2.0$ is shown in Fig. 18. The

result for the dilatancy parameter μ_1 = 0.0 is not presented in Fig. 17 as the difference between μ_1 = 0.0 and 0.1 is very minor.

It can be seen that by increasing the dilatancy parameter μ_1, the percentage of reduction of the load reaction in 1 direction will gradually increase. Furthermore, the larger ratios of the shear strain over the normal strain, the larger the dilatancy effect. This logical result indicates that the simple dilatancy model is able to properly estimate the influence of the dilatancy effect and can be employed in a more complex structure.

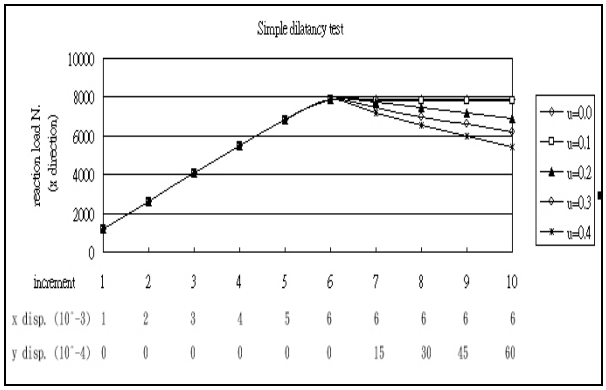

Fig. 17. Reaction load - load increment curve of simple dilatancy ($\frac{\Delta\gamma_{xy}}{\Delta\varepsilon_x} = 1.0$) (The symbol "u" represents dilatancy parameter (μ_1))

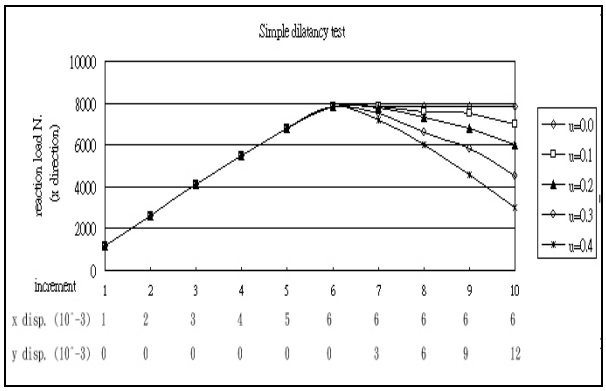

Fig. 18. Reaction load - load increment curve of simple dilatancy ($\frac{\Delta\gamma_{xy}}{\Delta\varepsilon_x} = 2.0$) (The symbol "u" represents dilatancy parameter (μ_1))

3.3 Single element test (III)

Following the previous dilatancy test, the shear displacement is increasing continually in the second step control until the reaction load becomes negative. This test is made to examine whether the compressive stress have been properly evaluated in the finite element implementation.

In this test, the ratio of shear strain over normal strain was chosen to be 35, i.e. $\frac{\Delta\gamma_{12}}{\Delta\varepsilon_{11}} = 35$, the dilatancy parameter μ_1 was chosen to be 0.4 and the result is shown in Fig. 19. In this study, the response of concrete under compressive stresses is assumed to be linear elastic until a so-called initial yield surface is reached. After that, the inelastic deformation begins and a work-hardening plasticity approach is employed for the irrecoverable part of deformation. Fig. 19 shows that the compressive stress has been properly evaluated.

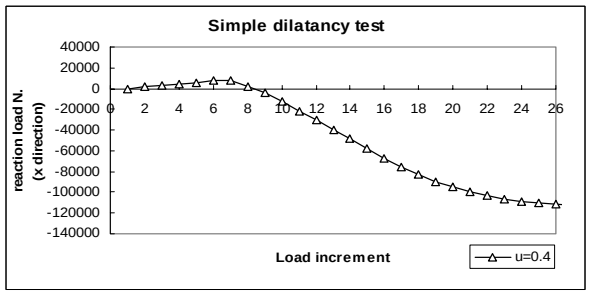

Fig. 19. Stress-strain relationship of simple dilatancy test

IV. CONCLUSION

The mechanical behaviour of the shear forces transfer to the cracked concrete is generally regarded to be very important aspect and will make significant effect on the whole behaviour in a structure. Most numerical applications adopt a so-called shear retention factor β to simulate the shear stress-shear strain relation in the crack development state. Moreover, due to the lack of experimental data, the magnitude of the shear retention factor β is generally assumed to be from 0 to 1. The interaction between the normal and shear displacement (or stress) is usually ignored. From the experimental evidence, it can be seen that the crack dilatancy effect is important to be taken into account in calculating the normal

and shear forces transfer to the cracked concrete. Therefore, when the dilatancy effect is not properly evaluated, it will affect the precision of the numerical prediction. However, very few of the crack models have incorporated the dilatancy effect in their crack models. Consequently, the influence of this effect in either the shear transfer in cracked concrete or in the whole structure is still not very clear. Therefore, it is very important to improve the understanding of its possible influence in the finite element application.

In this paper, a simple smeared crack dilatancy model is proposed. This model has incorporated the dilatancy effect and thus, a nonsymmetrical stiffness matrix is inevitably generated. Consequently, this leads to complicated programming and numerical instability. A single element test with displacement control has been carried out to validate the implementation. The logical result indicates that the simple dilatancy model is able to properly estimate the influence of the dilatancy effect and can be employed in a more complex structure.

NOTATION

The following symbols are used in this paper:

D_1 the stiffness modulus in 1 direction i.e. normal to the crack plane.

D_2 the stiffness modulus in 2 direction i.e. perpendicular to 1 direction.

Dcr cracked full D-matrix

D^{cr} stress-strain matrix for crack component

E Young's modulus

F yield function

f_t Uniaxial tensile strength

f_c' Uniaxial compressive strength (as a positive quantity)

f_1 The confinement normal stress

f_2 The shear stress

G_F Fracture energy

G $\dfrac{E}{2(1+\nu)}$ = Shear modulus

H' Hardening parameter

l_e Characteristic length

k_1 Dilatancy parameter

Δu_1 Normal displacement (mm)

Δu_2 Shear displacement (mm)

$\sigma_1, \sigma_2, \sigma_3$ Principal stresses, tensile positive

$\varepsilon_1, \varepsilon_2, \varepsilon_3$ Principal strains, tensile positive

$\Delta\tau_{12}$ Shear stress increment

$\Delta\gamma_{12}$ Shear strain increment

ν Poissons's ratio

Ω Element volume

σ_y Equivalent uniaxial yield stress

Q plastic potential function

$d\lambda$ The plastic multiplier

ε_p Equivalent total uniaxial plastic strain, $\varepsilon_p = \int (d\varepsilon^p d\varepsilon^p)^{1/2}$

dk Increment of plastic work

$\overline{\sigma}$ Equivalent uniaxial stress

σ_y^0 Initial yield stress

σ_{i+1} , σ_{i+2} stress in the two planes orthogonal to 'plane i'

ε_{11} total fracture strain in the first direction i.e. normal to the crack plane

ε_{22} total fracture strain in the second direction i.e. perpendicular to 1 direction.

ε_0 ultimate fracture strain

ε_t elastic ultimate strain

$\Delta\varepsilon_{11}^N$ Non-dilative concrete strain increment in

first direction

$\Delta\varepsilon_{22}^{N}$ Non-dilative concrete strain increment in the second direction

$\Delta\varepsilon_{11}^{D}$ Dilative concrete strain increment in the first direction

$\Delta\varepsilon_{22}^{D}$ Dilative concrete strain increment in the second direction

β Shear retention factor

μ Constant dilatancy parameter

REFERENCES

[1] Bazant, Z. P. and Cedolin, L., "Fracture mechanics of reinforced concrete." Journal of the Engineering Mechanics Division, ASCE, 106, pp. 1287-1306, 1980.

[2] Bazant, Z. P., and Oh, B. H., "Crack band theory for fracture of concrete." Materials and Structures RILEM, Vol.16, pp. 155-177, 1983.

[3] Cervera, M., Hinton, E., and Hassan,O., "Nonlinear analysis of reinforced concrete plate and shell structures using 20-noded isoparametric brick elements." Computers and Structures, Vol. 25, No. 6, pp. 845-869, 1987.

[4] Jefferson, A. D., and Wright, H. D., "Stepped softening function for concrete fracture in finite element analysis." Computers and Structures Vol. 41, No. 2, pp.331-344, 1991.

[5] Lotfi, H. R., and Shing, P. B., "An Appraisal of Smeared Crack Models for Masonry Shear Wall Analysis." Computers and Structures, Vol. 41, pp. 413-425, 1991.

[6] Feenstra, P. H., de Borst, R., and Rots, J. G., "Numerical study on crack dilatancy. I:models and stability analysis." Journal of Engineering Mechanics, Vol. 117, No. 4, pp. 733-753, 1991.

[7] Paulay, T., and Loeber, P. J., "Shear Transfer By Aggregate Interlock." ACI Special Publication SP 42-1 Detroit, Mich, pp. 1-15, 1974.

[8] Walraven, J. C., and Reinhardt, H. W., "Theory and Experiments on the Mechanical Behaviour of Cracks in Plain and Reinforced Concrete Subjected to Shear Loading." Heron, Vol. 26, No. 1a, pp. 5-68, 1981.

[9] Gambarova, P. G., and Karakoc,C., "A New Approach to the Analysis of the Confinement Role in Regularly Cracked concrete element." Trans. 7th Struct. Mech. in Reactor Tech.(SMiRT) Conf. H, pp. 251-261, 1983.

[10] Chan, A. H. C, Chuang, T. F., and Clark, L. A, "Preliminary Numerical Studies on Smeared Dilatancy Models on Nonlinear Finite Element," 6th ACME conference, Association for computational Mechanics in Engineering, pp. 23-26, England, 1998.

[11] Bazant, Z. P., and Gambarova, P., "Rough cracks in reinforced concrete." Journal of the Structural Division, ASCE, Vol. 106, No. ST4, pp. 819-842, 1980.

[12] Nilsson, L., and Oldenburg, M., "Non-linear Wave propagation in plastic fracture materials-a constitutive modeling and finite element analysis." IUTAM symp on Non-linear Deformation Waves, Tallin,

1982.

[13] Owen, D. R. J., Figueiras, J. A., and Damjanic, F., “Finite element analysis of reinforced and prestressed concrete structures including thermal loading.” Computer Methods in Applied Mechanics and Engineering Vol. 41, pp. 323-366, 1983.

[14] Kupfer, H. B., Hilsdorf, H. K., and Rusch, H., “Behaviour of concrete under biaxial stresses. Proceeding.” American Concrete Institute Vol. 66, No. 8, Aug., 656-666, 1969.

[15] Sinha, B. P., Gerstle, K. H., and Tulin, L. G., “Stress-strain relations for concrete under cyclic loading.” Journal of the American Concrete Institute February, Vol. 61, No. 2, pp. 195-211, 1964.

[16] FEA Ltd. Lusas User Manual, London, England, 2007.